

**Supplementary material of: Dynamic responses of community structure and
microbial functions of periphytic biofilms during chronic exposure to TiO₂ NPs**

Jun Hou^a, Tengfei Li^a, Lingzhan Miao^{a,*}, Guoxiang You^a, Yi Xu^a, Songqi Liu^a

^a Key Laboratory of Integrated Regulation and Resource Development on Shallow
Lake of Ministry of Education, College of Environment, Hohai University, Nanjing,
210098, People's Republic of China

*Corresponding author at: College of Environment, Hohai University, 1 Xikang Road.,
Nanjing 210098, People's Republic of China.

Email-address: lzmiao@hhu.edu.cn

Analyses of the microalgal composition

The PHYTO-PAM-II can excite chlorophyll fluorescence at five wavelengths (440, 480, 540, 590 and 625 nm) and automatically classify microalgae into four types (cyanobacteria, green microalgae, diatom and cryptophyta). A 5-min dark adaption was conducted prior to the determination. The fluorescence attributed to cyanobacteria, green alga, diatom and cryptophyta referred to Fo (Bl), Fo (Gr), Fo (Br) and Fo (PE-Type), respectively, which can represent the relative contribution of each microalgal group to the total community. The quantum yield was calculated as $(F_m - F) / F_m$, where F was the instantaneous fluorescence measured immediately after the application of a saturating light pulse and F_m was the basal fluorescence ¹.

High-throughput sequencing

E.Z.N.A.® Tissue DNA kit (Omega Bio-tek, Norcross, GA, U.S.) was used for DNA extraction according to the protocol. The quality of extracted DNA was detected by 1% agarose gel electrophoresis. Then the V4-V5 region of the bacterial 16S rRNA were amplified using the 338F and 806R primes and all quantitative amplifications were conducted in triplicate ². Then the PCR products were detected by 2% agarose gel electrophoresis and purified. Accurate quantitation of PCR products was performed with the QuantiFluor™-ST fluorometer (Promega, WI, U.S.). Sequencing libraries were generated using TruSeq™ DNA Sample Prep Kit (Illumina, CA, U.S.) following manufacturer's protocol. Finally, the bacterial communities were investigated by Illumina high-throughput sequencing.

Extraction and of EPS

1 g of wet biofilm sample was placed in 50 mL centrifuge tubes and mixed with distilled water to form a 50 mL suspension. After centrifugation at $6000 \times g$ for 10 min, the supernatant was removed and the sediments were re-suspended in a 0.05% (w/w) NaCl solution and sonicated at 20 kHz for 2 min. Then, the suspension was centrifuged at $8000 \times g$ for 10 min and the supernatant was collected as loosely bound EPS (LB-EPS). The residual sediments were re-suspended again with a 0.05% (w/w) NaCl solution and sonicated at 20 kHz for 2 min. After heating at $70 \text{ }^\circ\text{C}$ for 30 min, the suspension was finally centrifuged at $12,000 \times g$ for 20 min, and the supernatant was collected as tightly bound EPS (TB- EPS).

Table S1. Water quality parameters of Xuanwu Lake

| Parameter | □ |
|--------------------------|-----------|
| pH | 7.7 |
| dissolved organic carbon | 3.8 mg/L |
| total nitrogen | 2.3 mg/L |
| total phosphorous | 0.13 mg/L |
| ammonia | 0.62 mg/L |
| nitrate | 0.85 mg/L |

Table S2. Recipe of nutrient S1 (pH 7.8). Concentration of each component was provided in WC medium ³ and was diluted in nutrient S1.

| Component | Concentration |
|---|---------------|
| NaNO ₃ | 8.51 g/L |
| CaCl ₂ ·2H ₂ O | 3.676 g/L |
| MgSO ₄ ·7H ₂ O | 3.697 g/L |
| NaHCO ₃ | 1.26 g/L |
| Na ₂ SiO ₃ ·9H ₂ O | 2.842 g/L |
| K ₂ HPO ₄ | 871 mg/L |
| H ₃ BO ₃ | 2.4 g/L |
| Na ₂ EDTA·2H ₂ O | 109 mg/L |
| FeCl ₃ ·6H ₂ O | 78.75 mg/L |
| CuSO ₄ ·5H ₂ O | 62.5 µg/L |
| ZnSO ₄ ·7H ₂ O | 550 µg/L |
| CoCl ₂ ·6H ₂ O | 250 µg/L |
| MnCl ₂ ·4H ₂ O | 4.5 mg/L |
| Na ₂ MoO ₄ ·2H ₂ O | 157.5 µg/L |
| Na ₃ VO ₄ | 450 µg/L |
| Vitamin B12 | 6.75 mg/L |
| Thiamine | 16.75 mg/L |
| Biotin | 1.25 mg/L |

Table S3. Diversity estimates of bacterial communities in the controls, 50 $\mu\text{g/L}$ TiO_2 treatments and 500 $\mu\text{g/L}$ TiO_2 treatments. Data were expressed as the mean \pm standard deviation (n=4). All assays were conducted in four replicates, and significant differences between TiO_2 NP treatments were analyzed using one-way analysis of variance (ANOVA) using the SPSS software (V17.0). The p values below 0.05 were considered statistically significant.

| Sample | Shannon |
|--|----------------------|
| Control 7d | 4.3417 \pm 0.1249 |
| 50 $\mu\text{g/L}$ TiO_2 7d | 3.9302 \pm 0.0313* |
| 500 $\mu\text{g/L}$ TiO_2 7d | 3.8017 \pm 0.0795* |
| Control 14d | 4.2810 \pm 0.0459 |
| 50 $\mu\text{g/L}$ TiO_2 14d | 3.9977 \pm 0.3310 |
| 500 $\mu\text{g/L}$ TiO_2 14d | 4.0162 \pm 0.0214 |
| Control 21d | 4.8682 \pm 0.1241 |
| 50 $\mu\text{g/L}$ TiO_2 21d | 4.9420 \pm 0.0231 |
| 500 $\mu\text{g/L}$ TiO_2 21d | 4.9140 \pm 0.0677 |

*denotes a significant difference between the TiO_2 NPs treatments and the controls for $p < 0.05$.

Table S4. Effects of TiO₂ NP exposure on the bacterial communities in biofilms.

The eighteen dominant classes of bacterial communities were selected and their significant differences in relative abundances between the different treatments were estimated using one-way analysis of variance (ANOVA) using the SPSS software (V17.0). The *p* values below 0.05 were considered statistically significant.

| | Control 7d VS 50 µg/L TiO ₂ 7d | Control 7d VS 500 µg/L TiO ₂ 7d | Control 14d VS 50 µg/L TiO ₂ 14d | Control 14d VS 500 µg/L TiO ₂ 14d | Control 21d VS 50 µg/L TiO ₂ 21d | Control 21d VS 500 µg/L TiO ₂ 21d |
|----------------------------------|--|---|--|---|--|---|
| <i>Alphaproteobacteria</i> | 0.03 | 0.023 | 0.768 | 0.005 | 0.01 | 0.051 |
| <i>Cyanobacteria</i> | 0.143 | 0.005 | 0.167 | 0.268 | 0.312 | 0.79 |
| <i>Actinobacteria</i> | 0.084 | 0 | 0.067 | 0.009 | 0.494 | 0.487 |
| <i>Betaproteobacteria</i> | 0.025 | 0.141 | 0.046 | 0.627 | 0.076 | 0.014 |
| <i>Deltaproteobacteria</i> | 0.056 | 0.009 | 0.504 | 0.01 | 0.053 | 0.052 |
| <i>Gammaproteobacteria</i> | 0.218 | 0.497 | 0.824 | 0.77 | 0.995 | 0.211 |
| <i>Sphingobacteriia</i> | 0.069 | 0.105 | 0 | 0.003 | 0.24 | 0.022 |
| <i>Bacilli</i> | 0 | 0.001 | 0.002 | 0.003 | 0 | 0 |
| <i>Flavobacteriia</i> | 0.388 | 1 | 0.022 | 0.291 | 0.275 | 0.006 |
| <i>Cytophagia</i> | 0 | 0 | 0.121 | 0.17 | 0.116 | 0.012 |
| <i>norank p Saccharibacteria</i> | 0.902 | 0.044 | 0.862 | 0.832 | 0.898 | 0.003 |
| <i>Acidobacteria</i> | 0.09 | 0.078 | 0.71 | 0 | 0.042 | 0.038 |
| <i>Verrucomicrobiae</i> | 0.01 | 0.037 | 0 | 0 | 0.673 | 0.406 |
| <i>Gemmatimonadetes</i> | 0.326 | 0.022 | 0.447 | 0.173 | 0.151 | 0.052 |
| <i>Phycisphaerae</i> | 0.003 | 0.007 | 0.001 | 0.014 | 0.019 | 0.146 |
| <i>Chlamydiae</i> | 0.187 | 0.328 | 0.124 | 0.168 | 0.323 | 0.642 |
| <i>Chloroflexia</i> | 0.588 | 0.178 | 0.728 | 0.119 | 0.958 | 0.742 |
| <i>Bacteroidia</i> | 1 | 1 | 0.267 | 1 | 0.259 | 0.802 |

Table S5. Effects of TiO₂ NP exposure on the community variances assessed using Adonis and ANOSIM analysis with 999 random permutations.

| Paired samples | Adonis | | | Anosim | |
|--|--------|----------------|------|--------|------|
| | F | R ² | P | P | R |
| Control 7d_50 µg/L TiO ₂ 7d_500 µg/L TiO ₂ 7d | 7.9 | 0.72 | 0.01 | 0.01 | 0.74 |
| Control 7d_50 µg/L TiO ₂ 7d | 2.1 | 0.34 | 0.3 | 0.3 | 0.33 |
| Control 7d_500 µg/L TiO ₂ 7d | 46.3 | 0.92 | 0.1 | 0.1 | 1 |
| Control 14d_50 µg/L TiO ₂ 14d_500 µg/L TiO ₂ 14d | 7.8 | 0.72 | 0.01 | 0.01 | 0.67 |
| Control 14d_50 µg/L TiO ₂ 14d | 8.1 | 0.67 | 0.1 | 0.11 | 0.78 |
| Control 14d_500 µg/L TiO ₂ 14d | 14.3 | 0.78 | 0.1 | 0.11 | 1 |
| Control 21d_50 µg/L TiO ₂ 21d_500 µg/L TiO ₂ 21d | 2.51 | 0.45 | 0.03 | 0.01 | 0.31 |
| Control 14d_50 µg/L TiO ₂ 14d | 2.6 | 0.39 | 0.1 | 0.2 | 0.19 |
| Control 21d_500 µg/L TiO ₂ 21d | 6.3 | 0.61 | 0.1 | 0.09 | 0.85 |

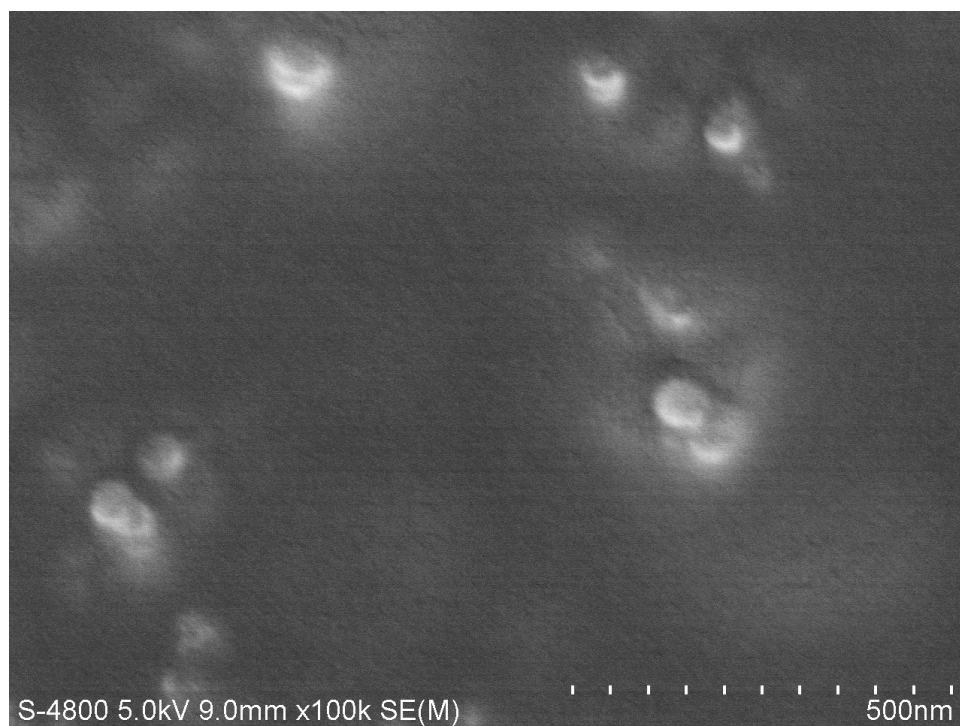


Figure S1. SEM image of commercial TiO₂ NPs.

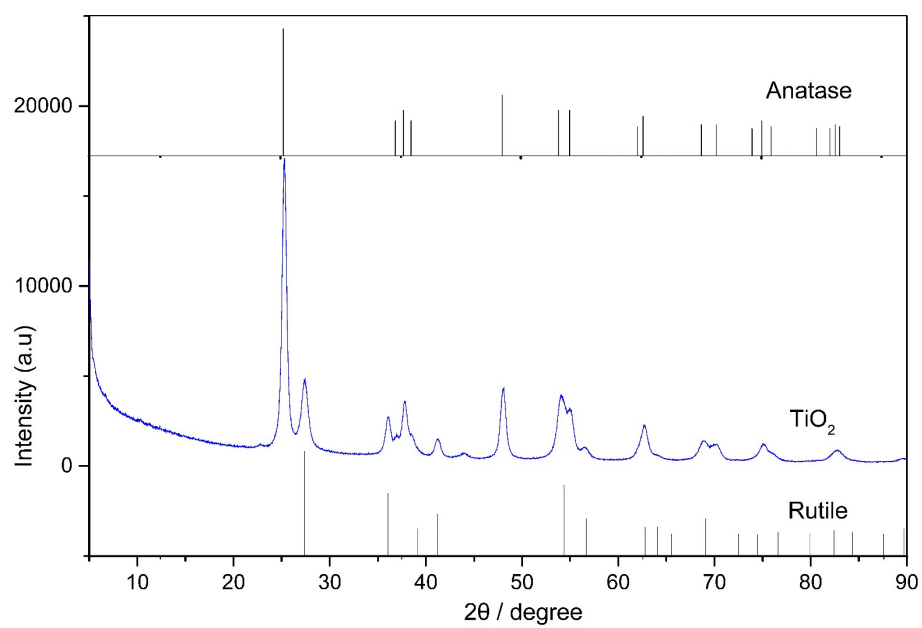


Figure S2. XRD pattern of commercial TiO₂ NPs.

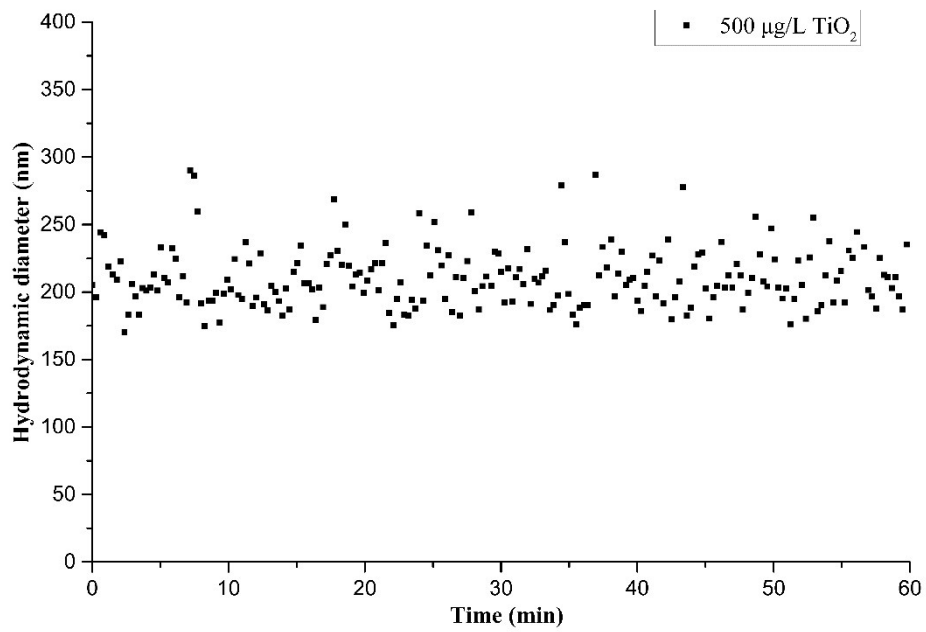


Figure S3. Changes in hydrodynamic diameters of 500 µg/L TiO₂ NPs in filtered culture medium.

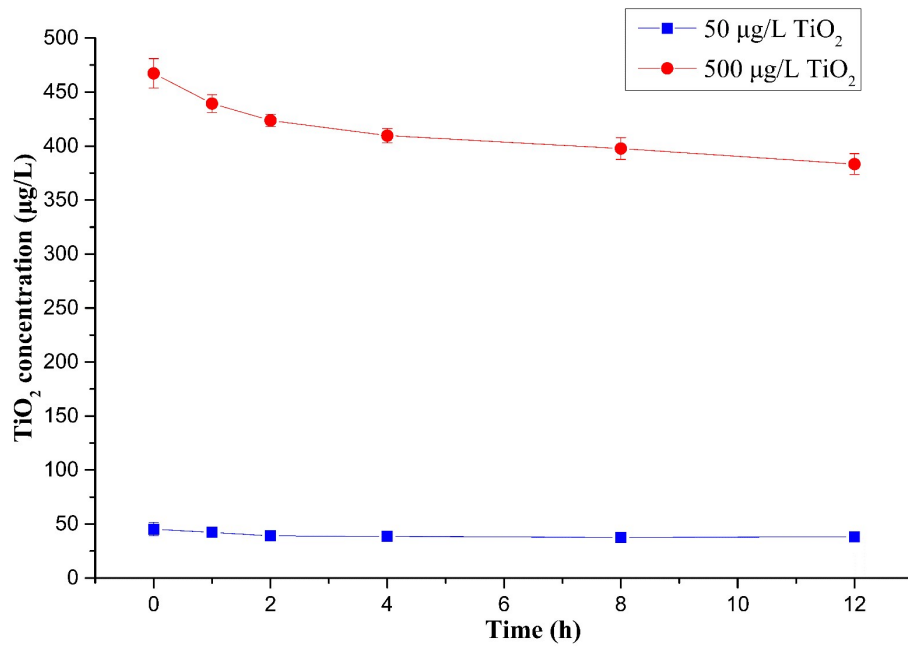


Figure S4. Changes in TiO₂ concentration in surface water. Error bars represent the standard deviation determined from measurements performed in triplicate.

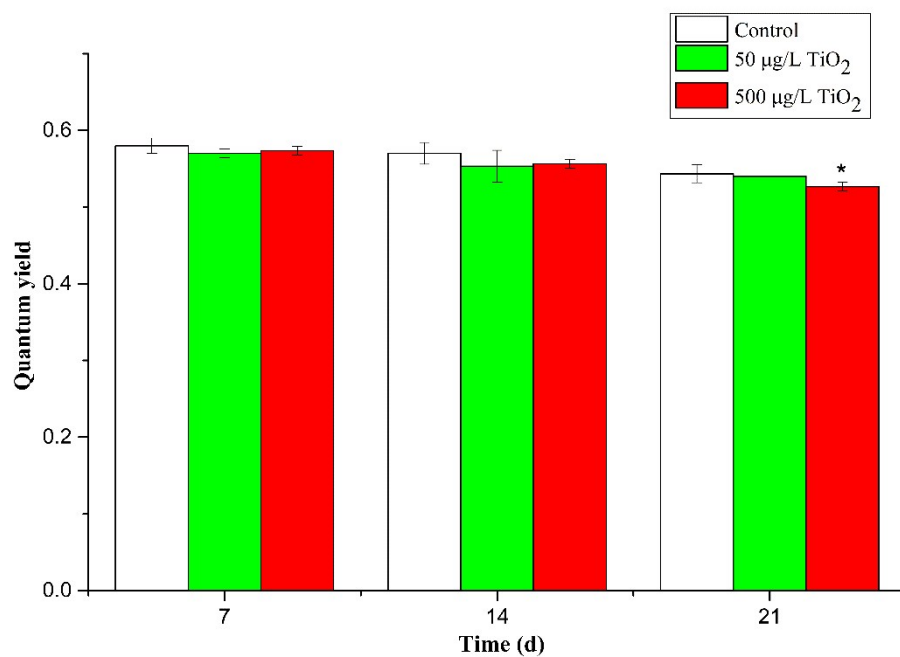


Figure S5. Effect of TiO₂ NP concentration on the quantum yield of periphytic biofilms at different times. * indicate statistical difference compared to the control ($p < 0.05$). Error bars represent the standard deviation determined from measurements performed in triplicate.

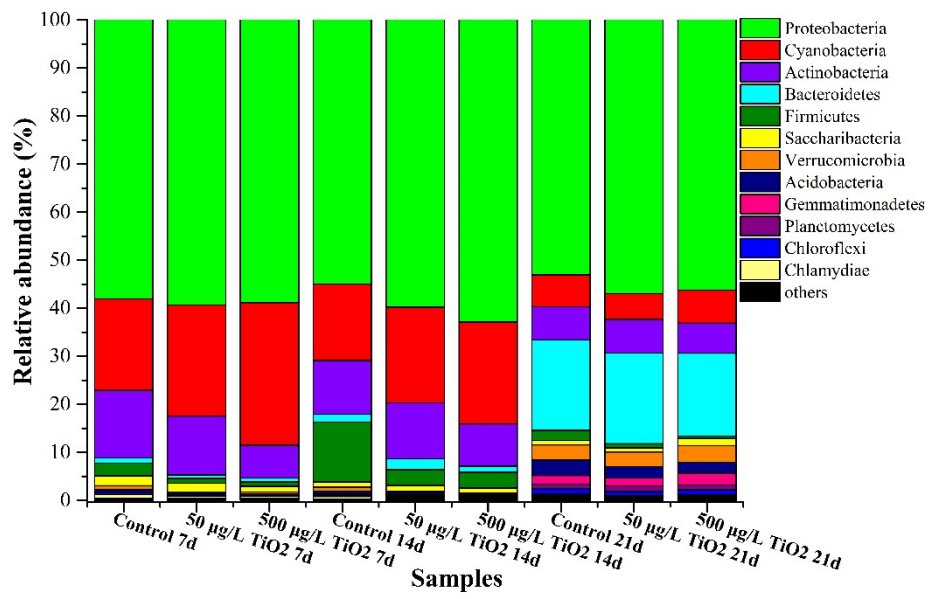


Figure S6. Relative abundance of dominant bacterial phylum in the microbial communities in all biofilm samples.

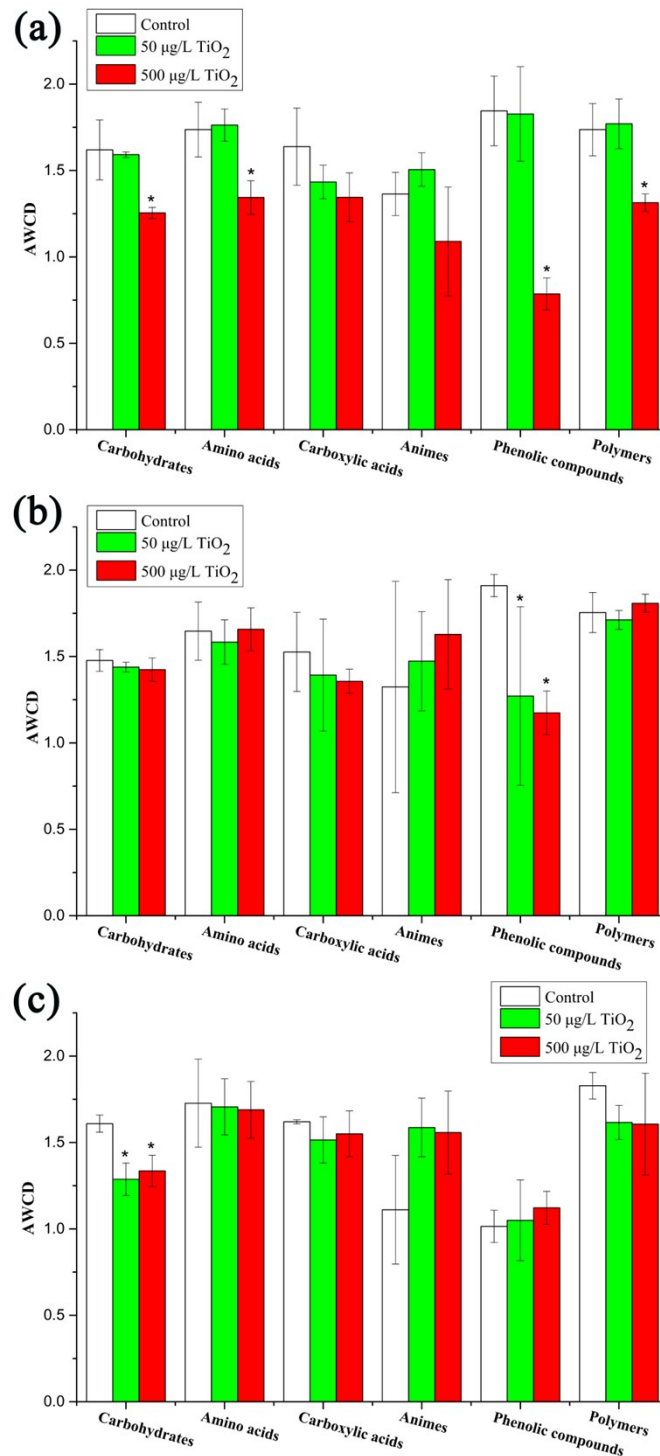


Figure S7. Effect of TiO₂ NP concentration on the microbial activity for six classes carbon substrates of periphytic biofilms at different times (7 day: a, 14 day: b, 21 day: c). * indicate statistical difference compared to the control ($p < 0.05$). Error bars represent the standard deviation determined from measurements performed in triplicate.

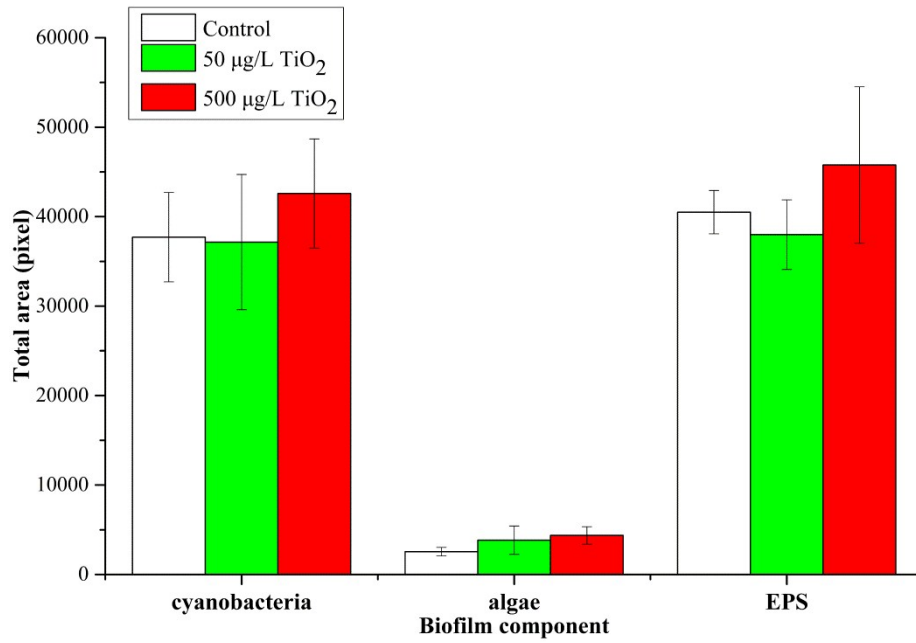


Figure S8. Quantitative analysis of CLSM images of periphytic biofilms under different treatment after exposure using Image J software. Error bars represent the standard deviation determined from measurements performed in triplicate.



Figure S9. Three flumes simulated the natural flow of water for exposure experiment.

Reference

1. Y. Xu, C. Wang, J. Hou, S. S. Dai, P. F. Wang, L. Z. Miao, B. W. Lv, Y. Y. Yang and G. X. You, Effects of ZnO nanoparticles and Zn²⁺ on fluvial biofilms and the related toxicity mechanisms, *Sci Total Environ*, 2016, **544**, 230-237.
2. N. Xu, G. C. Tan, H. Y. Wang and X. P. Gai, Effect of biochar additions to soil on nitrogen leaching, microbial biomass and bacterial community structure, *Eur J Soil Biol*, 2016, **74**, 1-8.
3. Y. H. Zhao, X. Xiong, C. X. Wu, Y. Q. Xia, J. Y. Li and Y. H. Wu, Influence of light and temperature on the development and denitrification potential of periphytic biofilms, *Sci Total Environ*, 2018, **613**, 1430-1437.